

## THE EFFECT OF SECOND PHASE PRECIPITATES ON THE WORK-HARDENING BEHAVIOUR OF ECAP-DEFORMED Al ALLOYS

E.F. Prados<sup>1</sup> V.L. Sordi<sup>2</sup>, M. Ferrante<sup>2</sup>

### ABSTRACT

A characteristic of metallic materials subjected to severe plastic deformation is a sharp decrease of work-hardening capacity. This reflects negatively on the ductility although there is some experimental evidence that ductility enhancing mechanisms can be activated. Among those, it appears that precipitates and dispersoids have some success, and the present study analyzes strength and work hardening behaviour of a ECAP-deformed Al-4%Cu alloy. Deformation was followed by a combination of precipitation/annealing heat treatments designed to produce a range of microstructures containing or formed by: (i) very large Al<sub>2</sub>Cu precipitates; (ii) small, peak strength precipitates; (iii) solid solution. Tensile test data of the various conditions were analyzed in conjunction with the corresponding microstructure. Results show that Al<sub>2</sub>Cu precipitates contributed to increase the work-hardening capacity of the Al-Cu system, either by increasing the dislocation density, or by pinning these defects and keeping them inside the grains, or both.

Keywords: ECAP; Al-Cu; precipitation; work-hardening.

1<sup>st</sup> TMS/ABM International Materials Congress  
July 25 - 30, 2010, Rio de Janeiro, Brasil

<sup>1</sup>PhD student, Federal University of São Carlos; <sup>2</sup> Professors, Federal University of São Carlos

## Introduction

It is well-known that one of the main problems of materials subjected to severe plastic deformation is limited ductility. From basic theory it is learned that the room temperature ductility of metals and alloys at low/medium strain rates is governed by a variety of factors. One of the most important is the work-hardening capacity (W-H); in the absence of this phenomenon, once attained yield stress, the stress-strain curve would be completely flat and elongation will be controlled by the necking rate. However this is rarely observed in coarse grained metals and alloys, since necking is delayed by W-H, which as a phenomenon was first treated by Taylor in 1934 [1]. Later, using only the average dislocation density ( $\rho$ ) as a state variable, Kochs [2] described W-H as a balance between dislocation multiplication induced by glide (A) and the annihilation of those defects (B):

$$\frac{d\sigma}{d\varepsilon} = A - B \quad (1)$$

- where A stands for  $k_1 \rho^{1/2}$ , with the constant proportional to the reciprocal of the mean free path of the moving dislocations. As for B it can be thought of as the "opposite counterpart" of dislocation accumulation and as such it must be analyzed in conjunction with this phenomenon. It acts by reducing the excess strain by the annihilation of dislocations of opposite sign.

These considerations are also valid for nanostructured materials, and since these have a very high proportion of atoms associated with the grain boundaries, intragranular-mediated plasticity is decreased, thus their low ductility. Moreover, in the particular case of highly deformed materials, residual stresses and dislocation locking are additional factors limiting ductility. Further, the small grain size and the easiness with which intragranular dislocation are attracted to the boundaries contribute to reduce the W-H capacity, thus the maximum strength ( $\sigma_u$ ) and the uniform elongation ( $\varepsilon_u$ ).

As mentioned, low ductility is the main drawback of nanostructured materials; however, some instances of ductile behaviour have been reported [3, 4], and the search for an explanation has led to the study of a number of mechanisms, one of which is based on precipitate/dislocation interaction. This mechanism affects positively the W-H rate and was originally treated by Ashby [5] and further extended by Estrin [6]. Their model suggests that dislocations storage around particles is relevant only for non-shearable precipitates. A good example of the role played by second phase precipitates is given by an investigation performed on an Al-Cu-Mg alloy, to which a combination of previous and post-deformation heat treatments gave a concurrent increase of strength and ductility [7]. Focussed on ductility improvement by precipitates, a thorough investigation was carried out by Cheng et al. on a commercial AA2024 alloy, which was cryo-rolled and subsequently aged at 100 and 160°C for different lengths of time [8]. Results show that the lower temperature precipitation heat treatment gave a good combination of strength and ductility, with elongation increasing by  $\approx 300\%$  with respect to the as-deformed material. This behaviour was attributed to dislocation accumulation around relatively large dispersoids combined with an increase of W-H rate. The latter effect was promoted by the nano-sized high volume fraction precipitates (10 to 15 nm;  $\approx 4 \times 10^{15} \text{ m}^{-2}$ ) produced by the 100°C heat treatment.

This paper presents some experimental results obtained on an Al-4%Cu alloy with different dispersion of Al<sub>2</sub>Cu precipitates. The main objective of the investigation was to characterize and discuss the relationship between the W-H behaviour and the dispersion parameters.

## Experimental

**1. Material:** a laboratory-cast Al-4%Cu alloy was conventionally extruded (40:1), and 14 x 14 x 70 mm<sup>3</sup> billets were machined from the bar.

**2. Deformation:** conducted at 25°C in an ECAP die with  $\Phi = 120^\circ$  and  $\Psi = 0^\circ$  (inner and outer radii of curvature equal to 8 mm). Specimens were subjected to one (1X) and to four (4X) passes following Route A.

**3. Heat treatment:** before deformation the billets were heated at 530°C/3 h. Part of the billets was water quenched from this temperature forming Group S, whilst the remaining was furnace cooled forming Group H. In part of the former group, post deformation heat treatment (PDHT) was conducted at 100°C/24 h and 170°C/2 h; identical thermal cycles were also employed for part of Group H. Figure 1 illustrates the solubilization → ECAP → PDHT sequence. A third condition, Cu in solid solution, was obtained by omitting the PDHT on Group S samples (1XS and 4XS). When not in use and before PDHT, all Group S billets were kept at subzero temperatures. Moreover, samples of billets 1XH and 4XH were left without PDHT.

**4. Characterization:** sub-sized tensile specimens (8 mm<sup>2</sup> section, 12 mm gauge length) were tested at 10<sup>-3</sup> s<sup>-1</sup> using an INSTRON machine Mod 5500R. Observation by transmission electron microscopy (TEM) was carried out in a Phillips CM 120 electron microscope. Foils were prepared by polishing 3 mm diameter discs until perforation in a TENUPO3 equipment and the electrolytic solution consisted of a 7:3 solution of methanol/nitric acid.

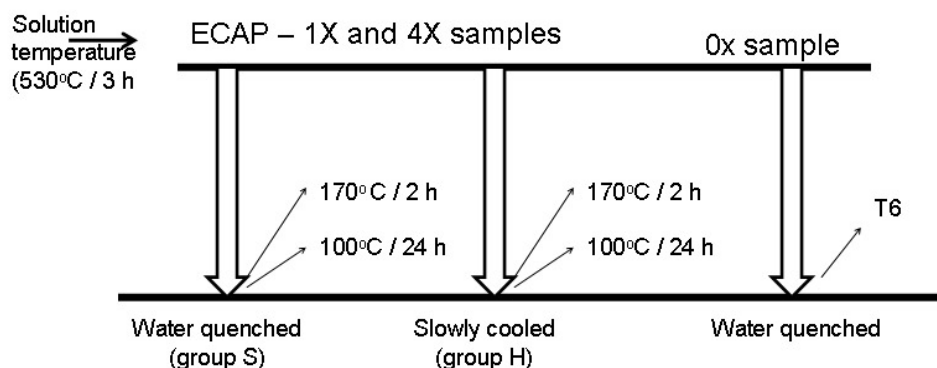


Figure 1. Schematic of the experimental procedure.

## Results and discussion

The heat treatments above described were applied with the purpose of obtaining two very different microstructures: (i) Group S begins as a solid solution, undergoes deformation, and precipitation takes place with full supersaturation; (ii) Group H is expected to display very large Al<sub>2</sub>Cu particles precipitated during the slow cooling.

Eventually, after PDHT, some precipitation may occur but to a lesser extent than in Group S due to the lower supersaturation. In short, PDHT is expected to be a proper precipitation thermal cycle for Group S, but mostly a dislocation anneal for Group H.

1. Tensile behaviour

The engineering stress strain curves for the two systems under various conditions are in Figure 2 and the respective quantitative data are summarized in Table 1.

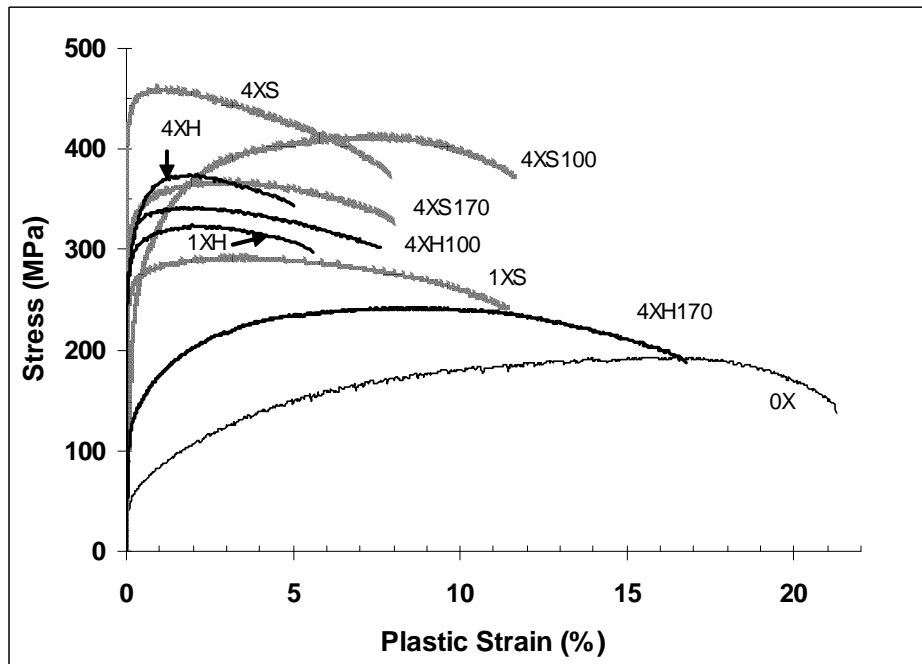


Figure 2. Engineering stress - strain curves of ECAP-deformed and heat treated Al-4%Cu alloy. Black lines - Group H; grey lines - Group S.

Table 1. Tensile properties and  $\sigma_u / \sigma_y$  ratio of ECAP-deformed and heat treated Al-4%Cu alloys

Sample	$\sigma_y$ (MPa)	$\sigma_u$ (MPa)	$\epsilon_u$ (%)	$\epsilon_t$ (%)	$\sigma_u / \sigma_y$
1XS	259	292	2.9	12	1.13
4XS	442	460	1,0	8.0	1.04
4XS (100)	280	413	8.0	12	1.48
4XS (170)	320	368	3.0	8.0	1.15
1XH	265	324	2.2	5.6	1.22
4XH	320	374	1.8	5.1	1.17
4XH(100)	310	342	1.8	7.6	1.10
4XH(170)	157	242	8.0	17	1.54
0X	75	220	14	--	2.93

From the above data, it can be observed that strength increases with the number of passes, as expected. Moreover, with the exception of specimen 4XH(170), Group S exhibits higher ductility, both uniform and total.

## 2. Microstructural development

Figure 3 shows typical features of the Al-4%Cu alloy after PDHT: micrographs (a) and (b) are representative of samples 4XS(100) and 4XS(170), respectively. It is apparent that the low temperature ageing resulted in dispersed, very small precipitates, whilst at 170°C the particles are much larger.

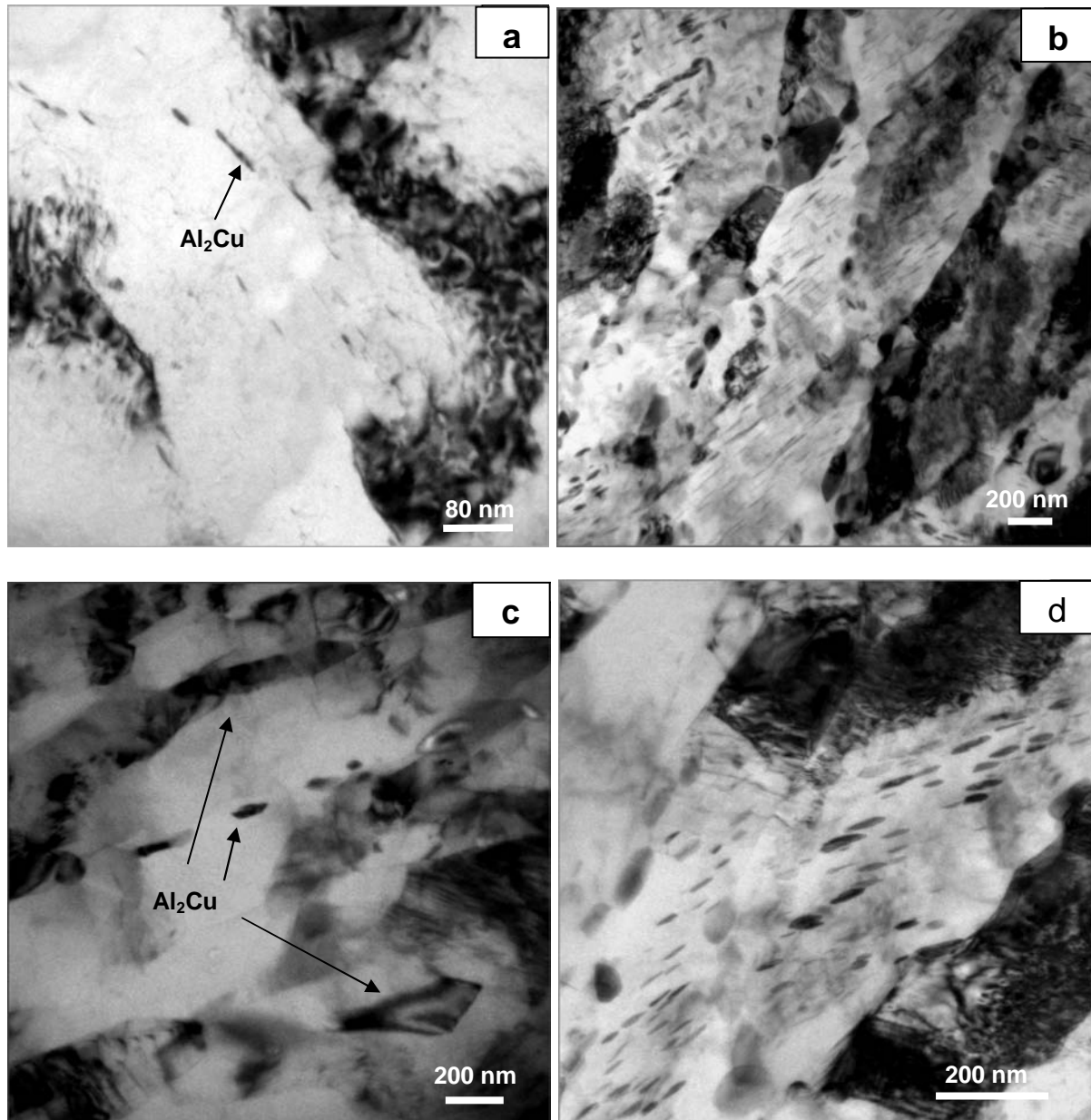


Figure 3. TEM micrographs of post-deformed heat treated samples: (a) 4XS(100); (b) 4XS(170); (c) 4XH(100) and (d) 4XH(170).

Table 2 contains the quantitative metallographic parameters for samples 1XS(100), 1XS(170), 4XS(100) and 4XS(170). Comparing the two samples submitted to four passes it is apparent that, if the average particle size increases 50% whilst the mean free path is halved, the 170°C PDHT led to more complete Al<sub>2</sub>Cu precipitation, in

other words, to a faster growth rate and a higher nucleation rate. As for the H Group, it was mentioned that the expected microstructure would be one composed almost entirely of large precipitates along the original grain boundaries. However, observing sample 4XH(100), see Figure 3-c, small and large precipitates coexist, suggesting that either the cooling rate from the solution temperature had not been slow enough, or that some of the large particles formed during the slow cooling were fractured by the shear deformation, an occurrence mentioned in the ECAP literature [9, 10]. The microstructure produced after high temperature PDHT of a 4XH sample is shown in Figure 3-d; again large and small precipitates coexist, but their density has increased suggesting more precipitation, thus implying that supersaturation was still present and that nucleation rate was higher.

More comments regarding the effect of severe deformation on precipitation are as follows:

(i) For the low temperature PDHT, Table 2 shows that increasing the deformation level of the S Group there is a concurrent increase of precipitates size and mean free path, indicating that deformation accelerates the coarsening rate, probably by a substructure effect. Indeed, in the presence of grain boundaries or low angle (dislocation) boundaries, precipitate coarsening follows a power law of the type [11]:

$$r^n - r_0^n = C t$$

- with n between 4 and 5 instead of n = 3 (matrix diffusion controlled coarsening).

(ii) The behaviour of Group H is difficult to rationalize due to the possibility of precipitate fracturing or even dissolution.

Table 2. Quantitative data on precipitate size (d), density ( $N_v$ ) and mean free path ( $\lambda$ )

Sample	d (nm)	$N_v$ ( $\mu\text{m}^{-3}$ )	$\lambda$ (nm)
1XS (100)	9.4 ± 0.4	26111	27
1XS (170)	34 ± 1.0	7701	46
4XS (100)	20 ± 2.0	--	65
4XS (170)	30 ± 2.0	--	37

It is now possible to analyze the relationship between uniform elongation and W-H behaviour as follows:

(i) PDHT causes different dynamic recovery rates when compared with the non-deformed (0X) and solid solution (1XS and 4XS) samples;

(ii) The results given by Group S in terms of the  $\sigma_u/\sigma_y$  parameter are very clear; precipitates increase the W-H ratio with respect to the solid solution samples 1XS and 4XS. Also, the higher the deformation level the lower the W-H rate, compare 1XS with 4XS. By exerting a dislocation pinning effect, the  $\text{Al}_2\text{Cu}$  particles can reduce the migration of said defects to the grain boundaries, thus decreasing dynamic recovery, or alternatively, increase the dislocation density by acting as Frank- Read sources.

(iii) The analysis of Group H is more complicated by the reasons already mentioned. At any rate, the presence of precipitates in samples 1XH and 4XH explains why their  $\sigma_u/\sigma_y$  parameters are larger than those of their Group S counterparts.

(iv) Sample 4XH(170) exhibits the largest W-H rate and ductility, but at the cost of very low strength but again, lack of quantitative data regarding precipitate dispersion makes difficult to understand its behaviour.

The literature contains evidence that shearable precipitates are less adequate for sustaining a high W-H rate since their efficiency for dislocation pinning is low [12, 13]. However, it is difficult to locate the shearable/non-shearable transition; for instance, Cheng et al state that the critical particle size ( $d_{cr}$ ) occurs after peak strength, that is, for the overaged condition [14]. On the other hand, Fazoli et al. found experimentally that  $d_{cr} = 3.7$  nm [13], a figure within the range 3 - 10 nm calculated by Hornbogen for partially coherent/incoherent  $Al_2Cu$  particles [15]. The present results seem to point to the right direction since precipitates are much larger than the figures above indicated, meaning that they certainly are of the non-shearable type.

## Conclusions

1. The best strength - ductility combination was obtained by the 100°C precipitation heat treatment of a sample which was ECAP-deformed in the solid solution condition.
2. The presence of  $Al_2Cu$  precipitates increases the W-H rate and uniform elongation of a ECAP-deformed Al-4%Cu alloy, particularly when PDHT is performed at low temperature (100°C).
3. Comparing samples 4XS with and without PDHT, it is apparent that the annealing effect is more accentuated than the hardening caused by precipitation; also, the 4XS(100) retains more W-H capacity than the 4XS(170).
4. Comparison of samples 1XS(100) with 4XS(100) shows that ECAP-deformation accelerates coarsening rate.
5. There are evidences of precipitate fracturing, although TEM observation of Group H samples show the permanence of large  $Al_2Cu$  particles, precipitated along grain boundaries during slow cooling.

## References

1. G.I. Taylor: Proc. Roy. Soc. Vol. A145 (1934), p. 362
2. U.F. Kocks: J. Eng. Mater. Technol. (ASME-H) Vol. 98 (1976), p. 76
3. Y. Wang, E. Ma and M.W. Chen: Applied Physics Lettrs. Vol. 80 (2002), p. 2395
4. A. Ma, K. Suzuki, Y. Nishida, N. Saito, I. Shigematsu, M. Takagi, H. Iwata, A. Watazu and T. Imura: Acta Mater. Vol. 53 (2005), p. 211
5. M.F. Ashby, in: *Strengthening Methods in Crystals*, edited by A. Kelly and R.B. Nicholson, John Wiley, New York (1971), p. 137
6. Y. Estrin, in: *Unified Constitutive Laws of Plastic Deformation*, edited by A.S. Krausz and K. Krausz, Academic Press, Orlando, FL (1996), p. 69

7. K.M. Hockauf, L.W. Meyer and L. Kruger: *Mat. Sci. Forum*, Vols. 584-586 (2008), p. 685
8. S. Cheng, Y.H. Zhao, Y.T. Zhu and E. Ma: *Acta Mater.* Vol. 55 (2007), p. 5822
9. M. Murayama, Z. Horita and K. Hono: *Acta Mater.* Vol. 49 (2001). p. 21.
10. C. Xu, M. Furukawa, Z. Horita and TG Langdon: *Acta Mater*, Vol. 53 (2005), p. 749
11. J. M. Martin, R.D. Doherty and B. cantor: *Stability of Microstructures in Metallic Systems*. Cambridge University Press, Cambridge (1997), p. 290:
12. S. Esmaeili, L.M. Cheng, A. Deschamps, D.J. Lloyd and W.J. Poole: *Mat. Sci. Eng.* Vols. A319-321 (2001) p. 461
13. F. Fazoli, W.J. Poole and C.W. Sinclair: *Acta Mat.* Vol. 56 (2008), p. 1909
14. L.M. Cheng, W.J. Poole, J.D. Embury, and D.J. Lloyd: *Metall. Mat. Trans.* Vol. 34A (2003), p. 2473
15. E. Hornbogen: *J. Mat. Sci.* Vol. 21 (1986), p. 3737